Science Advances

AAAS

advances.sciencemag.org/cgi/content/full/3/3/e1602552/DC1

Supplementary Materials for

Microbial arms race: Ballistic "nematocysts" in dinoflagellates represent a new extreme in organelle complexity

Gregory S. Gavelis, Kevin C. Wakeman, Urban Tillmann, Christina Ripken, Satoshi Mitarai, Maria Herranz, Suat Özbek, Thomas Holstein, Patrick J. Keeling, Brian S. Leander

Published 31 March 2017, *Sci. Adv.* **3**, e1602552 (2017)
DOI: 10.1126/sciadv.1602552

The PDF file includes:

- fig. S1. A synthesis of fundamental differences between the nematocysts in cnidarians and dinoflagellates.
- fig. S2. Ultrastructure and discharge of nematocysts in *P. kofoidii*.
- fig. S3. Nematocyst development in *P. kofoidii*.
- fig. S4. Nematocyst development in *Nematodinium* sp.
- fig. S5. Contractile and projectile traits in the nematocysts of *Nematodinium* sp.
- fig. S6. Molecular phylogeny of dinoflagellates with complex extrusomes.
- fig. S7. Model of nematocyst homology and evolution in dinoflagellates.
- fig. S8. Cytoskeletal associations with the nematocyst-taeniocyst complex in *P. kofoidii*.
- Legends for movies S1 to S5
- References (*40*–*44*)

Other Supplementary Material for this manuscript includes the following:
(available at advances.sciencemag.org/cgi/content/full/3/3/e1602552/DC1)

- movie S1 (.mpg format). FIB-SEM reconstruction of the nematocyst-taeniocyst complex in *P. kofoidii*.
- movie S2 (.mov format). Discharge of nematocyst isolated from *P. kofoidii*.
- movie S3 (.mpg format). Discharge of nematocyst isolated from *P. kofoidii*.
- movie S4 (.mpg format). *P. kofoidii* hunting *L. polyedra*.
- movie S5 (.mpg format). Discharge of a taeniocyst isolated from *P. kofoidii*.

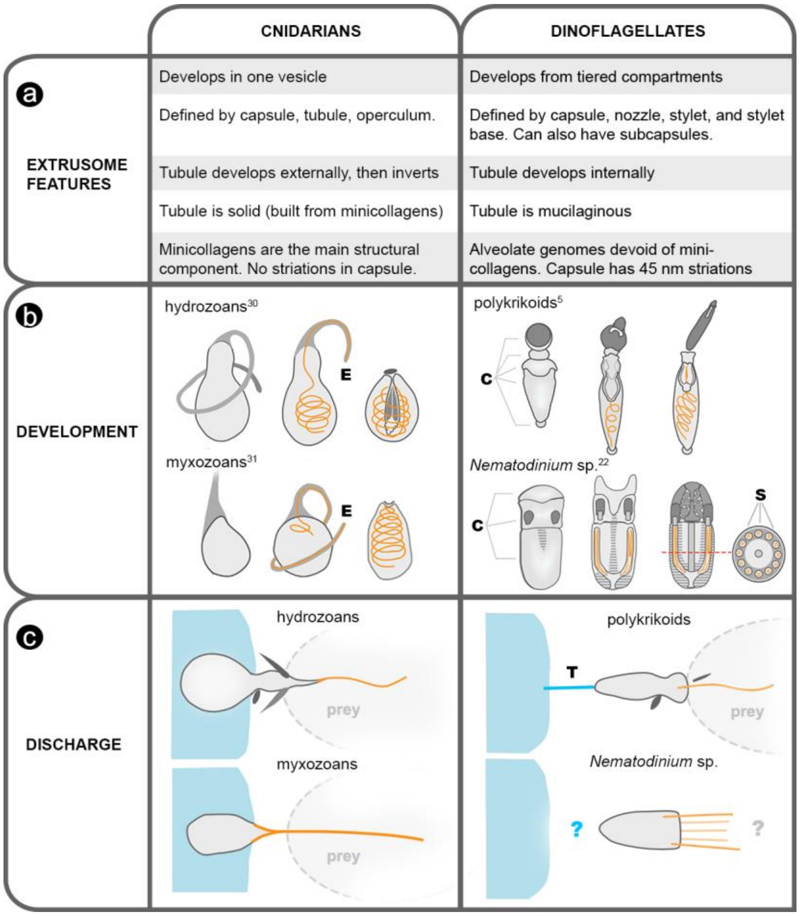

fig. S1. A synthesis of fundamental differences between the nematocysts in cnidarians and dinoflagellates. (**a**) A list of extrusomal features (with references given in *5*, *22*, *30*, *31*). (**b**) Illustrations of nematocyst development; tubules are orange, the dotted line in *Nematodinium* represents the plane of the cross section, on right. E = everting tubule. C = tiered compartments. S = subcapsules. (**c**) Illustrations of nematocysts firing. All illustrations are inferred from live observation except for that of *Nematodinium*, in which discharge has been only partially observed, in vitro. T = tow filament.

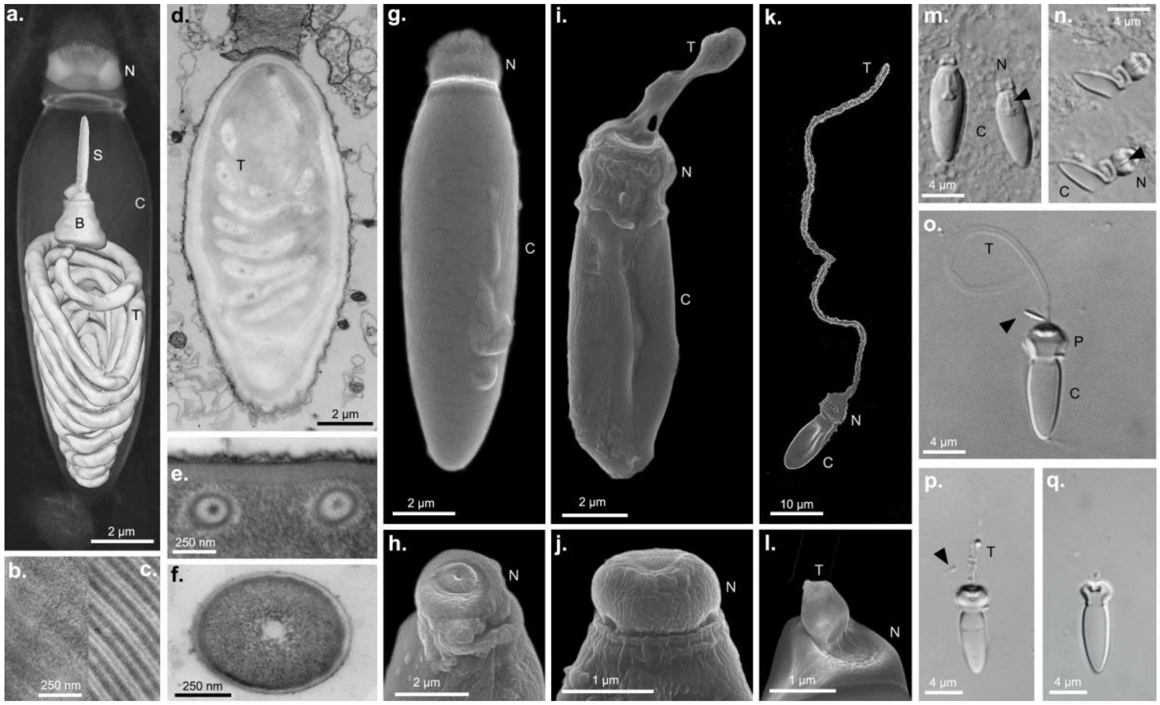

fig. S2. Ultrastructure and discharge of nematocysts in *P. kofoidii*. (**a**) FIB-SEM reconstruction of undischarged nematocyst with the tubule (T), stylet (S) and stylet base (B) rendered as a 3D surface, while the capsule (C) and nozzle (N) are overlaid as maximum intensity projections. (**b** and **c**) TEM sections of striated material found in the nematocyst capsule wall of *Polykrikos* (b) and *Nematodinium* (c). (**d**) Longitudinal TEM section of undischarged nematocyst. (**e** and **f**) Lateral TEM section of mucilaginous nematocyst tubules (e) compared to mucocyst (f)—another extrusome type found in *Polykrikos*. (**g–l**) SEM images of a resting nematocyst (g) and discharged nematocysts arrested in various stages of firing. (**m–q**) LM images of a resting nematocyst (m) and discharged nematocysts interrupted in various stages of firing showing the stylets (arrowheads) emerging along with a prolapsing part (P) of the capsule. The mucilaginous tubule begins to dissolve within 1 hr (p**)** and completely dissolves within 1 day (q).

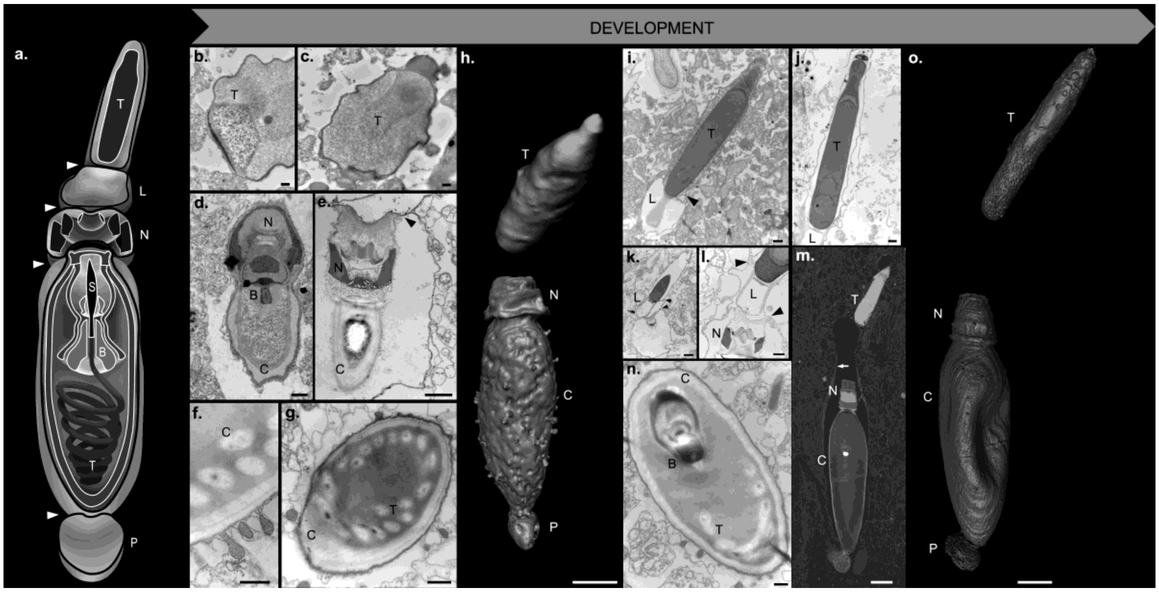

fig. S3. Nematocyst development in *P. kofoidii*. (**a**) Illustration of the nematocyst-taeniocyst complex; T = taeniocyst, L = linker, N = nozzle, S = stylet, B = stylet base, C = capsule, T = tubule and P = posterior compartment. Arrowheads show partitions between the five membrane-bound compartments. (**b**) Development of the nematocyst-taeniocyst complex. (**b** and **c**) Transmission electron micrographs (TEMs) of immature taeniocysts. (**d** and **e**) TEMs of an immature nozzle. (**f** and **g**) TEMs showing the developing capsule from vesicles containing granular contents. (**h**) 3D surface of an immature nematocyst-taeniocyst complex rendered from Focused Ion Beam SEM data (FIB-SEM). (**i** and **j**) Mature taeniocysts. (**k** and **l**) TEMs of a mature nozzle and linker. (**m**) FIB-SEM showing a maturing nematocyst-taeniocyst compartment. Most membranous partitions have fused to form a chute that encloses the nematocyst (arrow). (**n**) TEM of a mature capsule. (**o**) A 3D surface of the nematocyst-taeniocyst complex rendered from FIB-SEM data. Scale bars = 500 nm except in (f) (150 nm), and in (h, m, and o) (1 μm).

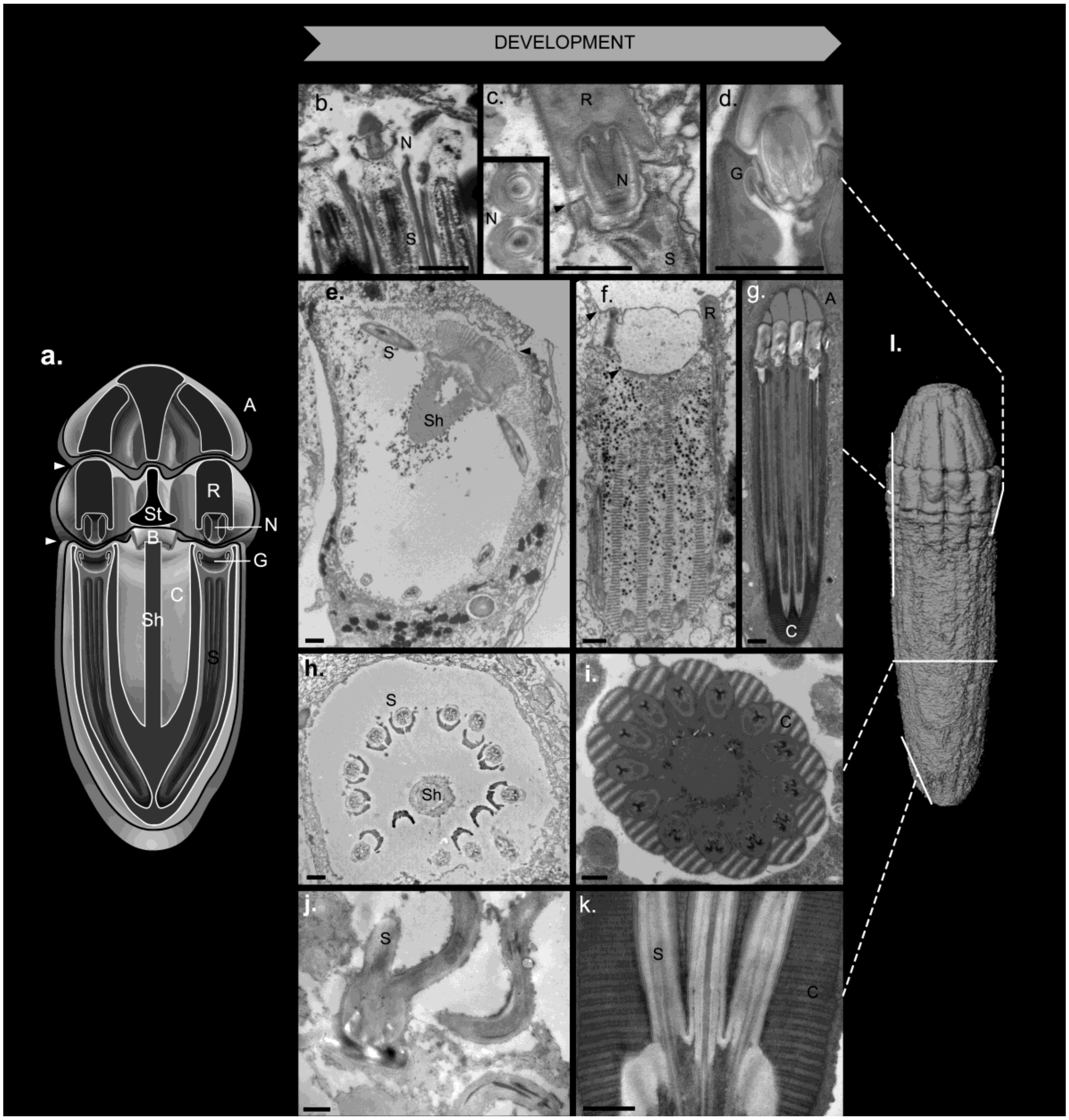

fig. S4. Nematocyst development in *Nematodinium* sp. (**a**) Illustration of the nematocyst; A = apical rosette, St = stylet, B = stylet base, R = rod, N = nozzle, G = gasket, C = capsule, Sh = shaft, and S = subcapsule. Arrowheads show partitions between the three membrane-bound compartments. (**b–k**) Transmission electron micrographs (TEMs) showing the development of the nematocyst. Development is defined by four major events: (1) three tiered compartments form; (2) internal structures differentiate; (3) nozzles become sealed; and (4): capsule wall hardens and takes on a striated appearance. (b–d) developing nozzles in longitudinal section, with inset in cross section. Each nozzle aligns with a gasket and subcapsule that seal together at maturity. (e–g) Capsule development in longitudinal section. (h and i) Capsule in cross section. The capsule is initially pliable, but becomes reinforced at maturity by the striated wall material. (j and k) Posterior of the nematocyst. The subcapsules are flexible, but become reinforced by striated material at maturity. (**l**) Focused ion beam scanning electron micrograph (FIB-

SEM) showing the surface of the nematocyst; lines indicate the planes of section from which the TEM images were produced. Scale bars = 1 µm.

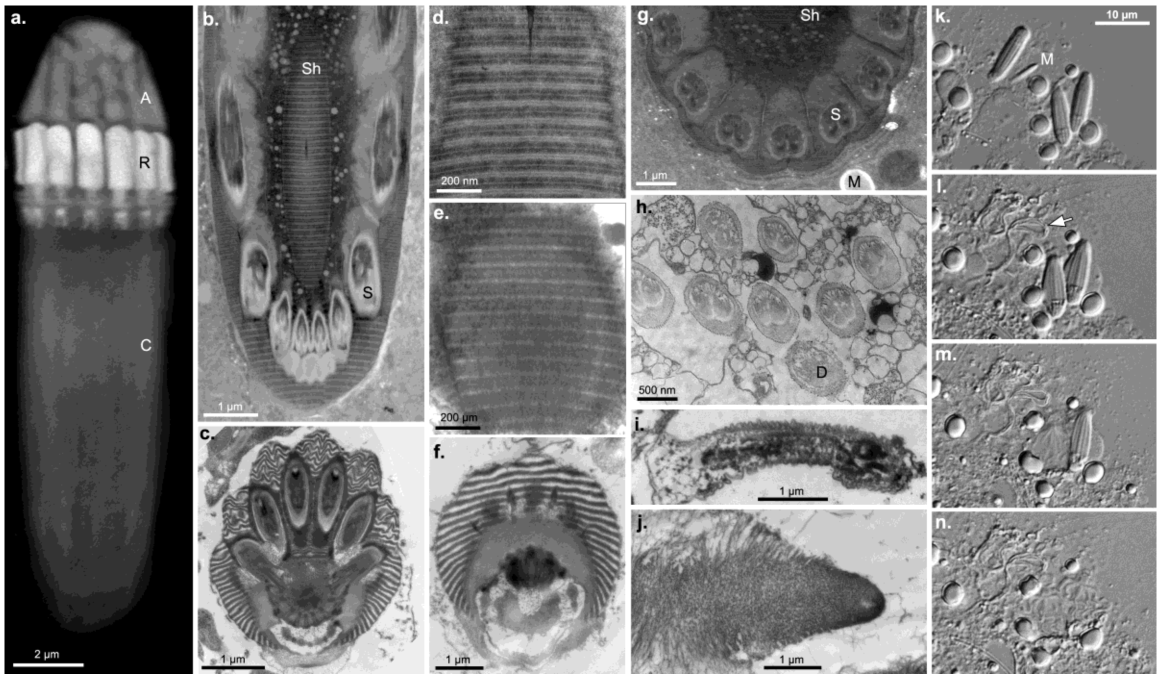

fig. S5. Contractile and projectile traits in the nematocysts of *Nematodinium* sp. (**a**) Maximum intensity projection of nematocyst from FIB-SEM showing apical rosette (A), rods (R), and capsule (C). (**b–f**) TEM sections of nematocysts in various stages of contraction as seen by the periodicity of their striated patterns. (b) Oblique view of relaxed nematocyst. (c) Oblique view of fully contracted nematocyst. (d) Relaxed striated matrix. (e) Partially contracted striated matrix. (f) Fully contracted striated matrix from proximal end of nematocyst. (**g**) Transverse section of nematocyst showing subcapsules (S) and shaft (Sh) beside a mucocyst (M). (**h**) A bundle of mucocyst-like extrusomes from cf. *Gymnodinium fasciculatum* called "docidosomes" (D), that resemble the subcapsules in *Nematodinium*. (**i**) Lateral view of a subcapsule that is being discharged in *Nematodinium* sp., enclosed in an accordion-like membrane. (**j**) Lateral view of a mucocyst being discharged. (**k**–**n**) Light micrographs across a 1.5 second time-series of isolated extrusomes from *Nematodinium* sp. as they spontaneously rupture/discharge. Arrow denotes the discharge of a mucocyst (M). All nematocysts have ruptured by the last frame. Once rupturing, subcapsules extend and become convoluted.

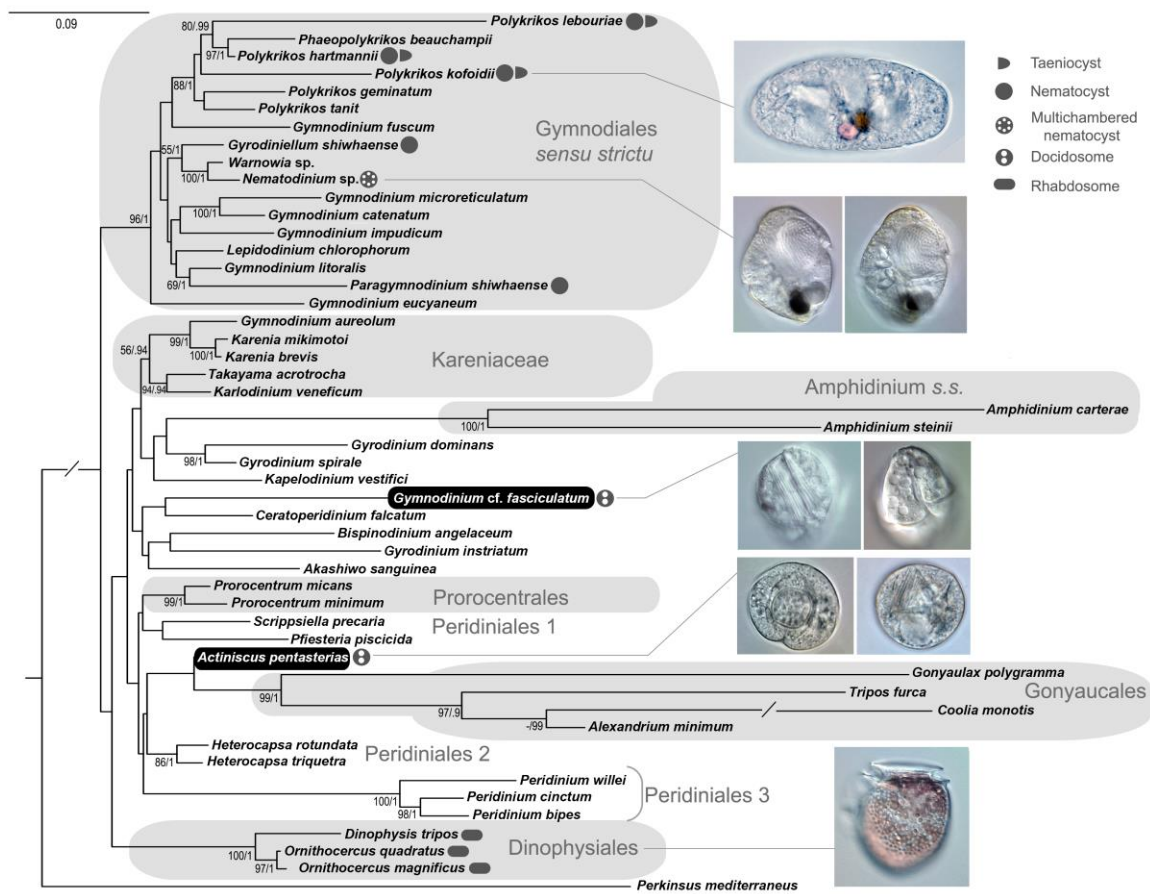

fig. S6. Molecular phylogeny of dinoflagellates with complex extrusomes. Multigene tree based on 18s and 28s rDNA sequences from across all sequenced dinoflagellates with nematocysts, as well as new sequences from dinoflagellates with complex extrusomes [*Actiniscus pentasterias* and c.f. *Gymnodinium fasciculatum*, both of which have “docidosomes” (*2*)]. The tree was inferred by analyzing a 50-taxon alignment (2,389 bp in length) using maximum likelihood. Statistical support for the branches was evaluated using 500 maximum likelihood bootstrap replicates and Bayesian posterior probability. Support values over 60/0.90 are shown. Light micrographs of extrusome-bearing species of dinoflagellates are shown on the right.

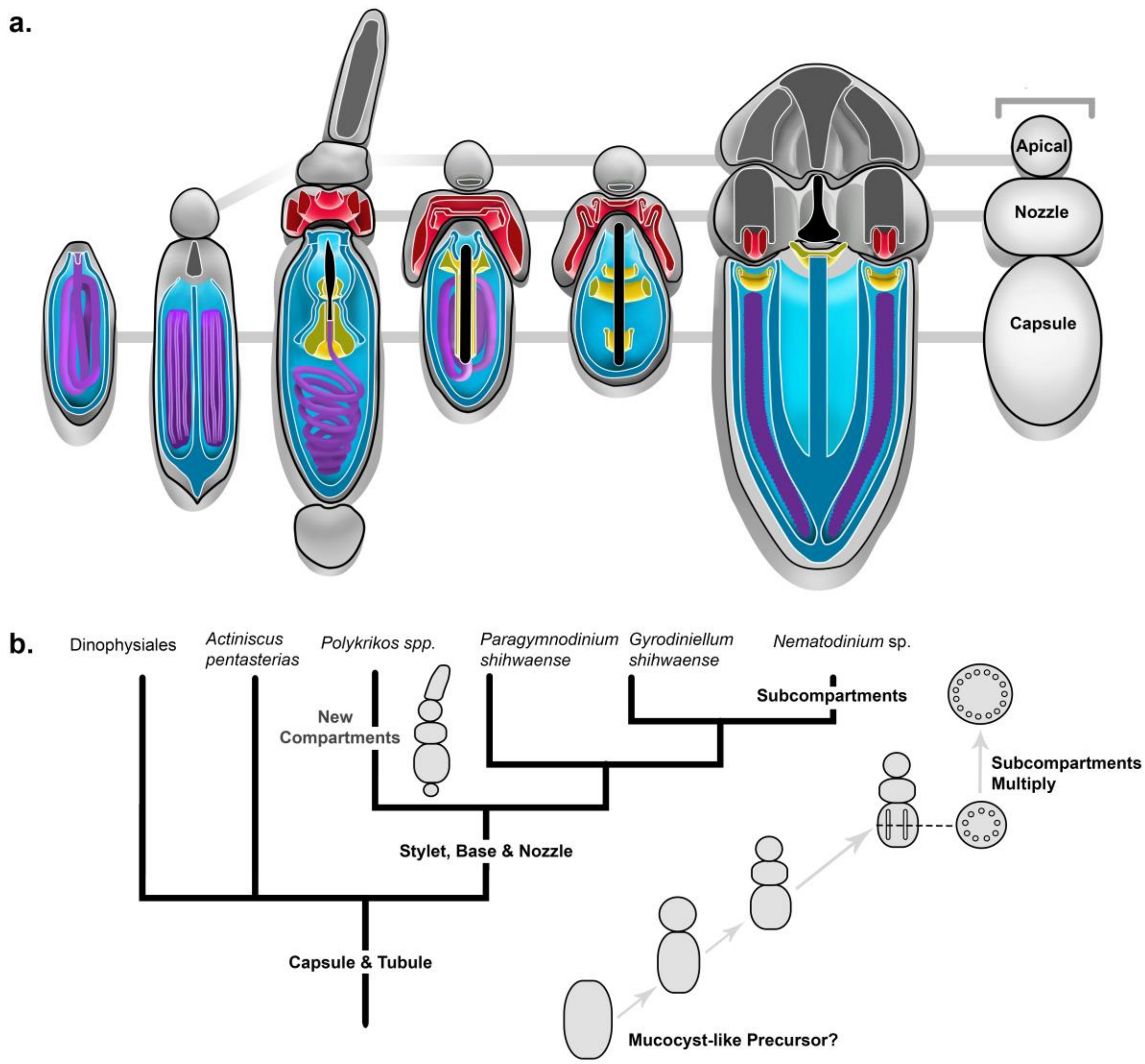

fig. S7. Model of nematocyst homology and evolution in dinoflagellates.
(**a**) Illustration of homologous components in the known nematocysts of dinoflagellates as inferred from single-cell focused ion beam scanning electron microscopy (FIB-SEM) and serial TEM sections (*15*, *22*, *30*, *43*, *44*). Colors indicate homology of specific components of nematocysts (red = nozzle, blue = capsule, black = stylet, yellow = stylet base, purple = tubule, grey = uncertain), and horizontal grey lines indicate homology between the major membrane-bound compartments. (**b**) Illustration of nematocyst traits mapped within a molecular phylogenetic context (based on fig. S6) showing the dinoflagellates with complex extrusomes. The number of major nematocyst vesicles/compartments is inferred to have increased over time along the lineage leading to polykrikoids (e.g., *Polykrikos*) and warnowiids (e.g., *Nematodinium*); the number of radially arranged subcompartments within nematocysts is inferred to have increased over time along the lineage leading to warnowiids (e.g., *Nematodinium* sp.).

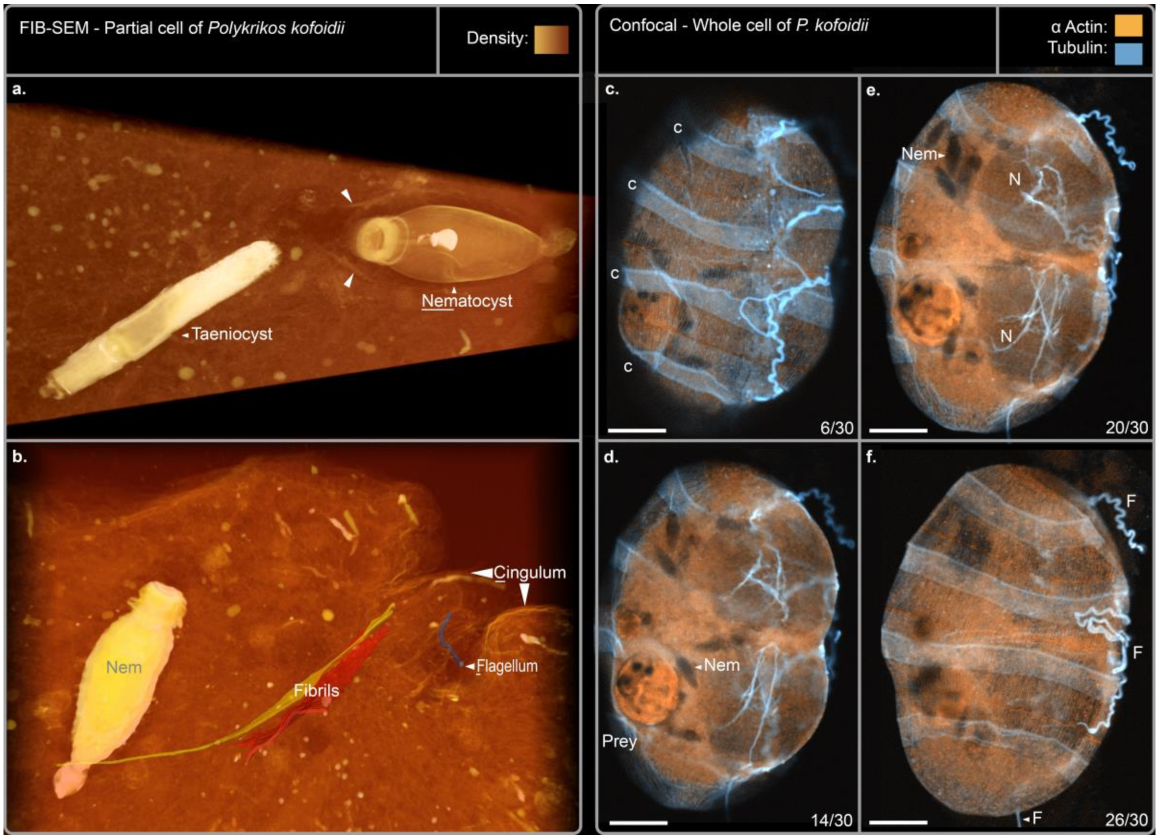

fig. S8. Cytoskeletal associations with the nematocyst-taeniocyst complex in *P. kofoidii*. (**a** and **b**) Focused ion beam scanning electron micrographs overlaid as 3D maximum intensity projections. (a) Nearly mature complex. Arrowheads = membrane of "chute" compartment. (b) Immature nematocyst, with two arrays of fibrils (colorized yellow and red) that lead to towards the cingulum, which is a lateral band along each segment of polykrikoids, bordering the flagellum (colorized blue). (**c–f**) Confocal laser scanning micrographs from an image stack of the whole cell. The position of each image in the 30-image stack is provided in the bottom right. Unlike the nematocysts of cnidarians, neither microtubules nor actin provide an extensive support network for the nematocysts in dinoflagellates. Nem = nematocyst, N = nucleus, F = flagellum, c = cingulum. Scale bars = 10 µm.

movie S1. FIB-SEM reconstruction of the nematocyst-taeniocyst complex in *P. kofoidii*. A stack of approximately 200 FIB-SEM sections is seen as a white maximum intensity projection, and specific nematocyst components have been colorized by manual segmentation in Amira. Purple = tubule; Dark blue = large ring of stylet base; Light blue = small ring of stylet base; Yellow = outer ring of nozzle; Orange = middle ring of nozzle; Red = innermost ring of nozzle.

movie S2. Discharge of nematocyst isolated from *P. kofoidii*. Differential Interference Contrast (DIC) light microscopy of a nematocyst isolated from a lysed cell.

movie S3. Discharge of nematocyst isolated from *P. kofoidii*. DIC light microscopy of a nematocyst isolated from a lysed cell.

movie S4. *P. kofoidii* hunting *L. polyedra*. DIC light microscopy of two prey capture events by *P. kofoidii.* In the first encounter, a *P. kofoidii* deploys both its nematocyst and taeniocyst to adhere to a prey cell. The nematocyst tubule is not seen as it is presumably injected into the prey. In the second encounter, the nematocyst tubule is discharged but glances off the prey. Still, the prey cell appears ensnared by *P. kofoidii* and is trawled behind the predator by a tow filament.

movie S5. Discharge of a taeniocyst isolated from *P. kofoidii*. DIC light microscopy of a taeniocyst, which was isolated from a lysed cell along with an associated nematocyst. The taeniocyst appears to spontaneously discharge its contents, suggesting that it is a ballistic organelle (an extrusome).